SIN-CHN SCIENTIFIC PRESS PTE.LTD.

Molecular & Cellular Biomechanics 2025, 22(4), 1475.
https://doi.org/10.62617/mcb1475

Article

Fe-doped polyoxometalates nanoclusters for near-infrared mild-temperature photothermal bacterial disinfection: A biomechanical perspective

Jing Zhou[1,2,†], Mingzhu Lv[2,3,†], Xinyi Wang[4], Yuan Yong[2,3], Guobo Du[2,*], Xiaoming Wang[1,2,*]

[1] Jinan University, No. 601, Huangpu Avenue West, Guangzhou 510630, China
[2] Affiliated Hospital of North Sichuan Medical College, Nanchong 637000, China
[3] Key Laboratory of General Chemistry of the National Ethnic Affairs Commission, School of Chemistry and Environment, Southwest Minzu University, Chengdu 610041, China
[4] North Sichuan Medical College, Fujiang Road 234, Nanchong 637000, China
*** Corresponding authors:** Guobo Du, duguobo@yeah.net; Xiaoming Wang, wangnsmc@163.com
[†] These authors contributed equally: Jing Zhou and Mingzhu Lv.

CITATION

Zhou J, Lv M, Wang X, et al. Fe-doped polyoxometalates nanoclusters for near-infrared mild-temperature photothermal bacterial disinfection: A biomechanical perspective. Molecular & Cellular Biomechanics. 2025; 22(4): 1475. https://doi.org/10.62617/mcb1475

ARTICLE INFO

Received: 30 January 2025
Accepted: 26 February 2025
Available online: 10 March 2025

Abstract: Currently, multidrug-resistant (MDR) pathogens are becoming a human and economic burden worldwide and have posed a grave threat to public health. In this case, mild-temperature photothermal therapy (PTT) has become a promising alternative to conventional antibiotics because it has the characteristics of minimally invasive property, targeted destructiveness, and low toxicity. To realize effective photothermal therapy, it is imperative to fabricate multifunctional photothermal formulations with better performance. In this study, novel Fe-doped polyoxometalate (Fe-POM) nanoclusters were successfully prepared by the one-pot method. Due to the strong absorption efficiency in the near-infrared (NIR) region, high photothermal conversion efficiency, and photothermal cycling stability, Fe-POM nanoclusters are sufficient to be used as an efficient photothermal agent for highly effective mild-temperature photothermal therapy. From a biomechanical perspective, the Fe-POM nanoclusters not only generate heat under NIR irradiation but also produce hydroxyl radicals (·OH) through the redox cycling of Fe^{2+}/Fe^{3+} and Mo^{5+}/Mo^{6+} pairs. The reactive oxygen species (ROS) generated disrupt bacterial cell membranes and alter their biomechanical properties, such as membrane stiffness and permeability, rendering the bacteria more susceptible to mild-temperature PTT. The synergistic effect of ROS-induced biomechanical stress and photothermal heating significantly enhances bacterial disinfection. Antibacterial experiments demonstrated that Fe-POM nanoclusters, under PTT conditions, effectively induce bacterial death while maintaining good biocompatibility. This study highlights the potential of Fe-POM nanoclusters as a multifunctional photothermal agent for combating bacterial infections. This work not only advances the field of photothermal therapy but also provides a novel strategy for treating bacteria-associated diseases through biomechanical modulation.

Keywords: polyoxometalate; mild-temperature photothermal therapy; biomechanical disruption; near-infrared region; bacterial infections

1. Introduction

Currently, more than 700,000 people die from bacterial infectious diseases annually, especially infections with multidrug-resistant (MDR) pathogens, and this is predicted to outnumber deaths caused by cancer [1]. As the pharmaceutical industry faces challenges in developing novel antibiotic formulations, there is an urgent need to develop novel non-drug approaches that can combat infections with drug-resistant bacteria [2]. Notably, photothermal therapy (PTT) based on near-infrared (NIR)

irradiation is a promising physical antimicrobial technology, which offers new ideas for avoiding drug resistance [3–5]. However, a major limitation of photothermal therapy is the undesirable damage and even inflammation to surrounding healthy cells and tissues caused by excess heat. This is especially unavoidable when high power (> 1 W/cm^2 for 1064 nm, 0.33 W/cm^2 for 808 nm) irradiation causes localized hyperthermia [6,7]. To overcome this limitation, PTT, which can cause bacterial damage at mild temperature, has received increasing attention in recent years due to its favorable biosafety [8–10]. However, as heat decreases, so does the bactericidal effect of PTT, which greatly hampers its use in clinical practice. With the rapid development of nanotechnology, nano drug delivery systems have become a hot research topic in the biomedical field. Such nano-scale systems precisely target tissues or cells, thus significantly improving drug targeting and bactericidal efficiency of PTT. The integration of biomechanical principles into nanomaterial design has opened new avenues for optimizing antimicrobial therapies. Biomechanical analysis provides crucial insights into how nanomaterials interact with bacterial cells at the cellular and molecular levels, particularly in terms of mechanical stress generation, membrane deformation, and cellular response to external stimuli. This biomechanical perspective is particularly relevant in the context of photothermal therapy, where the thermal effect of nanomaterials can generate mechanical stresses that enhance bacterial cell damage. In particular, the design of nano-drug delivery systems should not only consider the drug release mechanisms but also focus on biocompatibility and biodegradability to ensure that normal cells are not harmed during treatment.

Polyoxometalates (POMs) have emerged as a promising class of nanomaterials standing out from other photothermal agents due to their inherent advantages, including their ease of functionalization, reliable biocompatibility, ensuring minimal toxicity to biological systems, and desirable renal clearance, facilitating their elimination from the body [11,12]. These unique attributes have positioned POMs as front-runners in the field of nanomedicine. Previous studies have delved deeper into the multifaceted properties of POMs, revealing that in addition to their photothermal effects, they possess antibacterial properties. Specifically, POMs have been shown to induce bacterial membrane damage and trigger reactive oxygen species (ROS)-dependent oxidative stress in microorganisms. This dual mechanism of action enhances their antibacterial efficacy, making them potential candidates for combating antibiotic-resistant bacteria [13,14]. During the intricate process of ROS generation within the biofilm microenvironment (BME), POMs exhibit remarkable responsiveness to endogenous hydrogen peroxide (H_2O_2). Through the Fenton reaction, POMs catalyze the conversion of H_2O_2 into hydroxyl radicals (·OH), powerful oxidants known for their ability to disrupt biofilm structures and functions. However, despite their potential, the direct penetration of ROS within tissues remains a significant challenge due to biological barriers and tissue complexity [6]. In this context, biomechanical approaches offer promising solutions for enhancing ROS delivery. Recent advancements have demonstrated the application of external mechanical stimuli, such as photothermal, ultrasound, or magnetic fields, has been shown to enhance ROS diffusion and distribution within biofilms, potentially overcoming the limitations of passive diffusion. Although previous research has demonstrated the synergistic benefits of combining ROS-based therapies with

photothermal therapy (PTT), several limitations persist. One notable challenge is the potential damage caused by the excitation light used in PTT. This limits the irradiation exposure, thereby hindering the generation of sufficient ROS levels required for therapeutic efficacy. As such, achieving an optimal synergistic effect between mild PTT and ROS-based therapies remains both challenging and crucial. Overcoming these limitations will pave the way for the development of more effective and safe nanomedicine platforms utilizing POMs.

In this study, we successfully synthesized multifunctional molybdenum-based polyoxometalate nanoclusters (designated as Fe-POM) that were strategically doped with iron through a straightforward one-pot method. This innovative synthesis aimed to harness the unique properties of Fe-POM for enhanced ROS generation within the near-infrared II (NIR-II) biological window at mild temperatures, thereby facilitating photothermal therapy (PTT). Moreover, we explored the biomechanical applications of Fe-POM, such as how its structure and composition can be optimized for behavior within cells. From a biomechanical perspective, the iron doping in Fe-POM not only enhances its catalytic properties but also modifies its mechanical characteristics. The distinctive composition of Fe-POM imparted it with the remarkable capability to serve as an efficient ROS generator, producing hydroxyl radicals (·OH) via a Fenton-like reaction. Notably, these ROS generation processes could be further augmented by localized photothermal effects, creating a synergistic interaction. In turn, the enhanced photothermal effect facilitated deeper penetration of ROS into bacterial cells, exacerbating their susceptibility to damage. Furthermore, when applied to bacterial cultures, Fe-POM treatment induced a massive and rapid burst of ROS, leading to the accumulation of malondialdehyde (MDA), a biomarker of oxidative stress. This oxidative stress made the bacteria highly vulnerable to mild-temperature PTT, significantly enhancing the antimicrobial efficacy of the treatment. From a biomechanical perspective, we also assessed the impact of Fe-POM on bacterial biofilms, finding that it effectively disrupted the integrity of biofilms, thereby enhancing antibacterial activity. The mechanical disruption of biofilms by Fe-POM was attributed to a combination of factors, including the material's ability to generate localized mechanical stresses, its interaction with extracellular polymeric substances (EPS), and its capacity to alter the viscoelastic properties of the biofilm matrix. Importantly, at concentrations effective for antimicrobial activity, Fe-POM exhibited minimal impact on the viability of cells in normal tissues, indicating its specificity for bacterial targets and suggesting a favorable safety profile. Ultimately, this innovative approach effectively eliminated bacteria while demonstrating excellent biocompatibility, underscoring its potential as a promising therapeutic strategy. We eagerly anticipate that this Fe-POM-based antimicrobial approach will pave the way for promising clinical translations, offering a novel and efficacious solution to combat bacterial infections. The integration of biomechanical principles into the design and application of Fe-POM represents a significant advancement in antimicrobial therapy. By combining the chemical and photothermal properties of POMs, this approach offers a multifaceted strategy for combating drug-resistant bacteria. Future research directions could explore the optimization of Fe-POM for specific applications, such as implant coatings or wound dressings, where controlled mechanical interactions with bacterial biofilms could enhance therapeutic outcomes. Additionally, the development

of advanced biomechanical models to predict and optimize the interactions between Fe-POM and bacterial cells could further improve the efficacy and safety of this promising antimicrobial platform.

2. Results and discussion

2.1. Synthesis and characterization of Fe-POM

The Fe-POM nanoclusters, exhibiting a dark blue and transparent appearance, were meticulously synthesized through a straightforward one-pot method [6,15]. This method involved the strategic doping of Fe ions into the framework of Mo-based polyoxometalate nanoclusters, followed by a reduction process facilitated by L-ascorbic acid. The synthesis process was carefully optimized to ensure the uniform distribution of Fe ions within the nanoclusters, which is crucial for their functional properties. As visualized by the transmission electron microscopy (TEM) image (**Figure 1A**), the as-synthesized Fe-POM nanoclusters displayed a remarkable uniformity and well-dispersed granular nanostructure, indicative of their high quality and potential for further applications. The consistent morphology of these nanoclusters not only enhances their stability but also improves their interaction with target cells, making them suitable for biomedical applications. In addition, the average hydrodynamic diameter of these Fe-POM nanoclusters, as recorded by dynamic light scattering (DLS) measurement, was approximately 10.1 nm (**Figure 1B**). This precise sizing further underscores their potential for effective interaction with biological systems. Such a small size is particularly beneficial for cellular uptake, allowing the nanoclusters to penetrate biological membranes more easily. Furthermore, the Fourier transform infrared (FTIR) spectrum provided additional affirmation, revealing specific absorption peaks derived from the inherent structure of POMs, thereby confirming the successful incorporation of Fe ions into the Mo-based nanoclusters (**Figure 1C**). In addition, we have conducted the powder X-ray diffraction (XRD) analysis to investigate the crystal structure of Fe-POM. As depicted in **Figure 1D**, we note that the XRD pattern of Fe-POM exhibits significant peak broadening, resulting in peak overlap and low signal intensity that causes great difficulty in discerning characteristic diffraction peaks. The result attributes to the unique PXRD property of nanoscale materials that decreasing crystalline domain size in nanoscale causes more noticeable peak broadening [16]. This is consistent with our findings that Fe-POM has ultrasmall morphology with a nanoscale crystalline domain size. To rigorously evaluate the stability of the Fe-POM nanoclusters, changes in their hydrodynamic diameter and zeta potential in aqueous solutions were meticulously recorded over a period of 7 days. As presented in **Figure 1E**, these measurements demonstrated no significant changes during this timeframe, clearly indicating the excellent stability of Fe-POM for long-term storage and potential use in various applications. This stability is essential for ensuring the reliability of the nanoclusters in therapeutic settings, where prolonged circulation time can enhance their efficacy. Notably, the negatively charged Fe-POM nanoclusters possess an ultra-small hydrodynamic size, which is advantageous for their rapid removal from the body without causing serious adverse effects on healthy tissues. Furthermore, the chemical states in Fe-POM have been evaluated using X-ray photoelectron spectroscopy (XPS) analysis, revealing the

presence of elements C, O, Fe, and Mo (**Figure 1F**). Notably, high-resolution Fe 2p and Mo 4d spectra confirmed the co-existence of multivalent Fe (+2 and +3) and Mo (+5 and +6) in Fe-POM (**Figure 1G,H**). This characteristic further supports their potential as a safe and effective therapeutic agent in clinical applications.

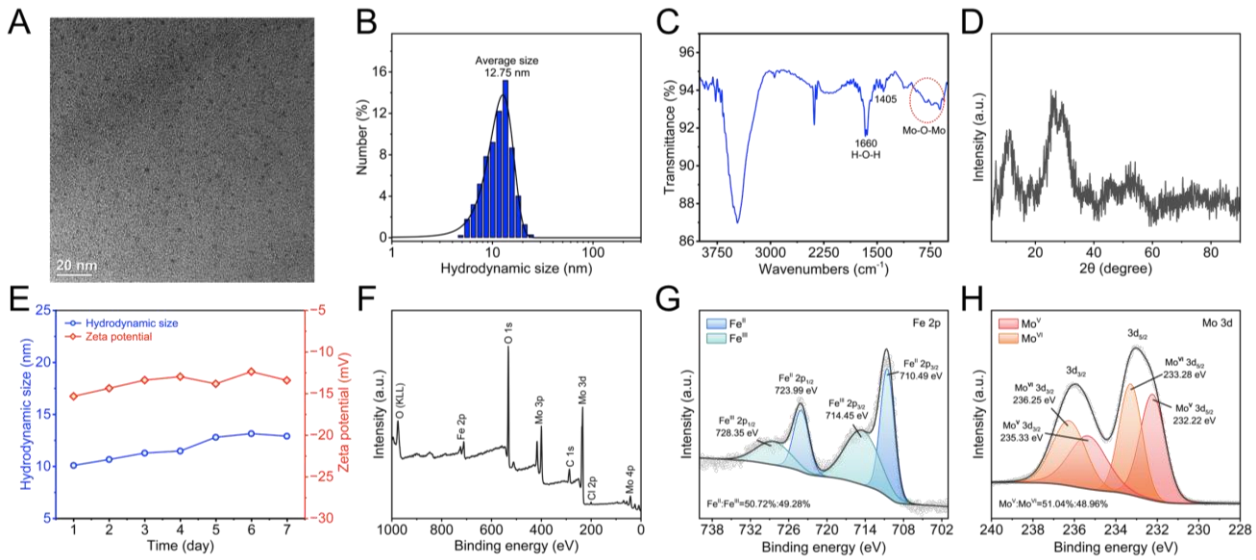

Figure 1. Characterizations of Fe-POM nanoclusters. **(A)** TEM image of Fe-POM nanoclusters; **(B)** hydrodynamic diameter of Fe-POM nanoclusters; **(C)** Fourier transform infrared (FTIR) spectrum of Fe-POM nanoclusters; **(D)** XRD patterns of Fe-POM nanoclusters; **(E)** the hydrodynamic size and zeta potential of Fe-POM nanoclusters in aqueous solution at different times; **(F)** XPS spectra of survey scan of Fe-POM; XPS spectrum of **(G)** Fe 2p and **(H)** Mo 3d.

Importantly, the UV-vis absorption spectra provided further insights into the optical properties of Fe-POM nanoclusters. These spectra verified a rather broad absorption efficiency throughout the near-infrared (NIR) region. This exceptional absorption capability can be attributed to the electron relaxation polarization resulting from charge transfer between reduced Mo^{5+} and oxidized Mo^{6+} species, facilitated by bridging oxygen bonds within the nanocluster structure (**Figure 2A**). This unique optical property endows Fe-POM nanoclusters with great potential for photothermal applications. Moreover, as the concentration of Fe-POM aqueous solutions was increased from 50 to 300 μg/mL, the absorption intensities in both the NIR-I and NIR-II bio windows gradually increased in a linear relationship. This linear relationship between absorption intensities and Fe-POM concentration, as depicted in **Figure 2B,C**, further highlights their potential as quantitative photothermal agents. Overall, these comprehensive results not only confirm the successful preparation of Fe-POM nanoclusters but also underscore their great potential for serving as efficient photothermal agents in various biomedical applications.

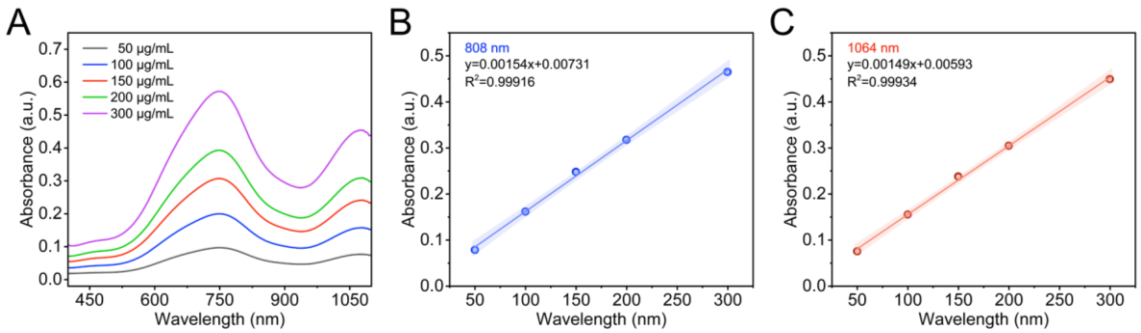

Figure 2. (A) UV-vis spectra of Fe-POM aqueous solution with various concentrations. Calibration curve of absorbance at **(B)** 808 nm and **(C)** 1064 nm vs. concentration of Fe-POM aqueous solution.

2.2. Photothermal conversion performance of Fe-POM

Next, encouraged by the impressive absorption capabilities of the as-prepared Fe-POM in the near-infrared (NIR) region, we decided to delve deeper into their photothermal conversion behaviors, specifically at wavelengths of 808 nm and 1064 nm, respectively. When Fe-POM aqueous solutions were irradiated with either an 808 nm laser or a 1064 nm laser, the entire system underwent rapid heating through the efficient photothermal energy conversion of the incident light. This conversion process was not only swift but also highly effective, demonstrating the potential of Fe-POM for photothermal therapy (PTT) applications. As shown in **Figure 3**, Fe-POM exhibited a concentration-dependent, irradiation time-dependent, power density-dependent, and pH-dependent temperature elevation in both the NIR-I (808 nm) and NIR-II (1064 nm) regions. Notably, after 15 min of irradiation at the same Fe-POM concentration, the temperature increase observed in the NIR-I region was notably higher than that in the NIR-II region. This finding underscored the superior photothermal conversion capacity of Fe-POM across the entire NIR spectrum, with particularly impressive performance in the NIR-II region. This superior performance in the NIR-II region suggested the exciting possibility of utilizing Fe-POM in PTT for deeper tissue penetration, given that NIR-II light has better tissue penetration capabilities compared to NIR-I light [17].

To further validate the practicality of Fe-POM for PTT applications, we assessed its photothermal stability by illuminating its aqueous solutions (100 μg/mL) over four repeated heating/cooling cycles. Encouragingly, after four cycles, the temperature of the Fe-POM aqueous solutions could still reach the temperature peaks achieved in the previous cycles, indicating their remarkable and consistent photothermal stability. This was clearly evident from the temperature profiles presented in **Figure 3C,F**, which demonstrated minimal deviation in peak temperatures across the four cycles. Overall, these findings highlighted the promising potential of Fe-POM for photothermal therapy applications, particularly in the context of deeper tissue penetration.

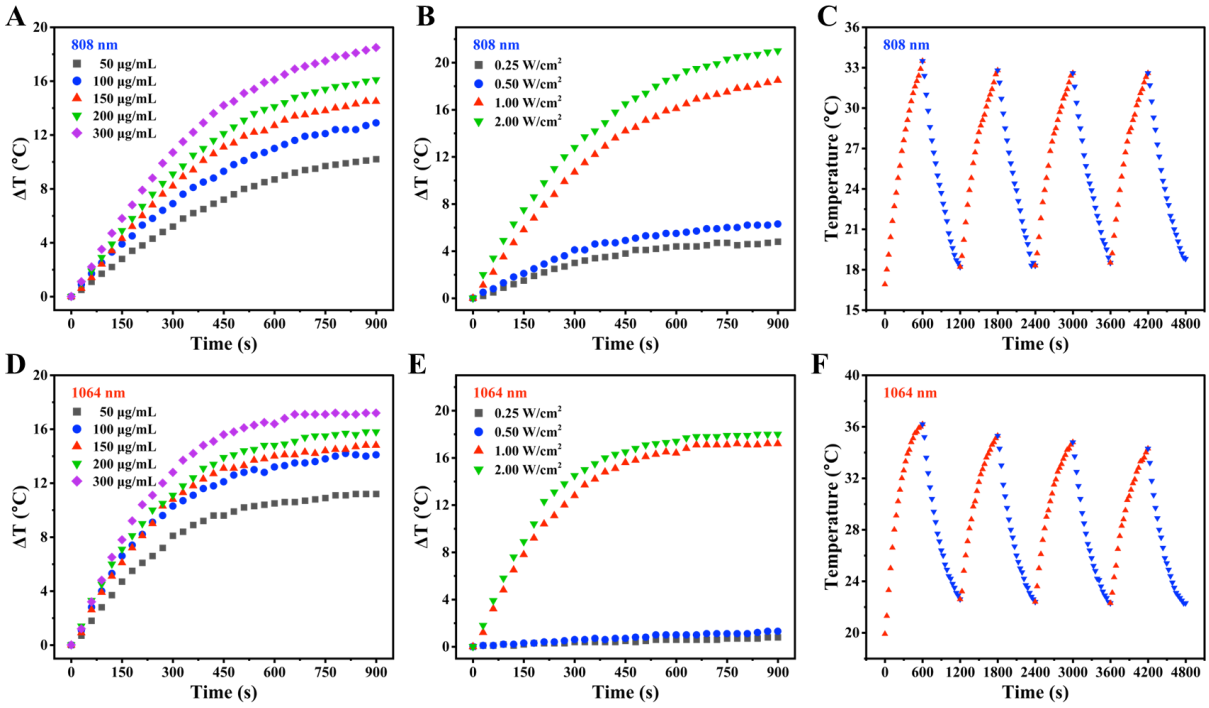

Figure 3. Photothermal conversion performance of Fe-POM. The temperature vs. time curves of different concentrations of Fe-POM under **(A)** 808 nm and **(D)** 1064 nm laser irradiations. The temperature *vs.* time curves of Fe-POM under **(B)** 808 nm and **(E)** 1064 nm laser irradiations at different power densities. The temperature *vs.* time curves of Fe-POM over **(C)** 808 nm and **(F)** 1064 nm laser on/off cycles.

2.3. Catalytic properties of Fe-POM

To further validate Fe-POM as an effective reactive oxygen species (ROS) generator for chemodynamic therapy (CDT), we conducted experiments to assess its ·OH generation activity using two indicators: methylene blue (MB) and 3,3′,5,5′-tetramethylbenzidine (TMB). Specifically, the ability of Fe-POM to catalyze a Fenton-like reaction in the presence of H_2O_2 was evaluated. This evaluation is crucial, as the generation of ·OH radicals is a key mechanism by which CDT exerts its therapeutic effects. As shown in **Figure 4**, when Fe-POM was introduced into the reaction system containing H_2O_2, it effectively catalyzed the Fenton-like reaction, leading to the generation of ·OH radicals. These radicals subsequently induced the degradation of MB, as evidenced by the decreasing absorbance of the MB characteristic absorption peak at 664 nm. This decrease in absorbance was concentration-dependent, with increasing concentrations of Fe-POM (ranging from 0 to 200 μg/mL) leading to more pronounced degradation of MB (**Figure 4A**). In addition to MB, we also used TMB as an indicator to further confirm the ·OH generation activity of Fe-POM. When TMB was treated with Fe-POM alone, only a slight increase in absorbance was observed at TMB's characteristic absorption peak (652 nm) (**Figure 4B**). However, when NIR irradiation was applied in combination with Fe-POM, a significant increase in absorbance was observed at the characteristic peaks. This result confirmed that photothermal therapy (PTT) enhanced the CDT effect of Fe-POM by promoting the generation of ·OH radicals. Overall, these findings provided strong evidence supporting the effectiveness of Fe-POM as an ROS generator for CDT applications.

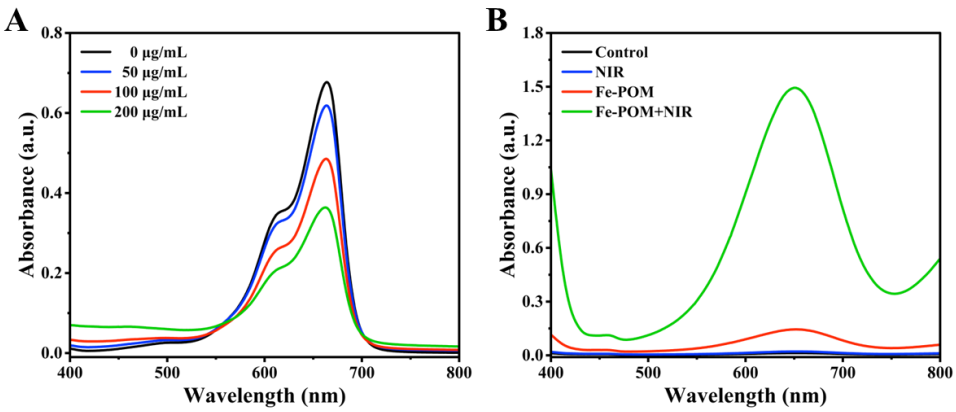

Figure 4. (A) MB degradation by Fe-POM nanocluster-mediated Fenton-like reaction with different concentrations (0–200 μg/mL); **(B)** UV-vis spectra of TMB oxidation under different treated conditions.

2.4. In vitro antibacterial activity of Fe-POM

Fe-POM is anticipated to induce bacterial vulnerability by generating an abundance of ROS through its dual enzyme-like activities, ultimately enhancing the subsequent efficacy of mild-temperature photothermal therapy (PTT). To rigorously investigate this hypothesis, a series of experiments were conducted using methicillin-resistant Staphylococcus aureus (MRSA) as the model bacterium. Initially, MRSA was co-incubated with Fe-POM for a duration of 2 h to allow for sufficient interaction and ROS generation. Subsequently, the bacteria were subjected to NIR irradiation at a power density of 1.0 W/cm^2 for 10 min. This step was crucial to assess the combined effect of Fe-POM-based mild-temperature PTT and chemodynamic therapy (CDT) against MRSA. Following the NIR irradiation, the antimicrobial efficacy of the treatment was evaluated using the standard agar plate assay. As shown in **Figure 5**, the results revealed that NIR treatment alone, without the presence of Fe-POM, did not exhibit prominent antimicrobial activity. This indicated that the NIR irradiation itself was not sufficient to inhibit bacterial growth. On the other hand, when MRSA was treated with Fe-POM alone, only a slight inhibition effect on bacterial proliferation was observed. This suggested that while Fe-POM had some antibacterial activity, it was not sufficient to completely eradicate the bacteria. However, under 808 nm NIR irradiation (1.0 W/cm^2, 10 min) in the presence of Fe-POM, a moderate antibacterial effect was noted. This indicated that the combination of Fe-POM-mediated CDT and mild PTT at this wavelength had a synergistic effect, enhancing the antibacterial activity. Furthermore, when MRSA was pretreated with Fe-POM and subsequently irradiated with a 1064 nm laser (1.0 W/cm^2, 10 min), the bacteria lost the ability to form bacterial colonies on the agar plate. This dramatic result demonstrated the excellent antimicrobial effect of Fe-POM-mediated mild PTT at this wavelength, further validating the hypothesis that Fe-POM can enhance the efficacy of mild-temperature PTT through its dual enzyme-like activities and ROS generation.

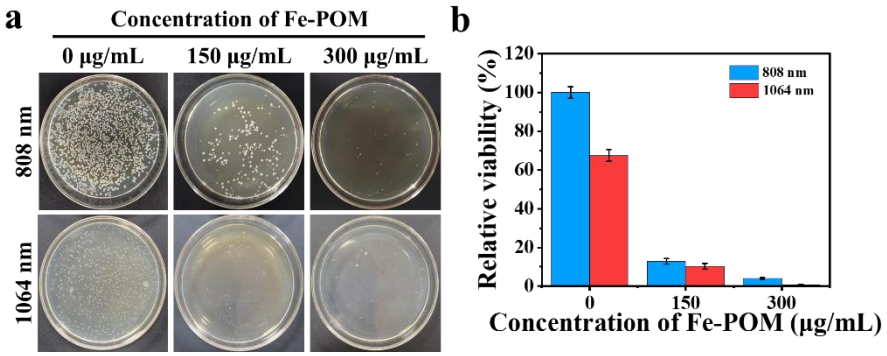

Figure 5. (a) Photographs of bacterial colonies and **(b)** the corresponding quantitative analysis of MRSA upon different treatments.

3. Materials and methods

3.1. Materials

Ammonium molybdate tetrahydrate ($(NH_4)_6Mo_7O_{24}\cdot 4H_2O$), iron chloride hexahydrate ($FeCl_3\cdot 6H_2O$), L-ascorbic acid were purchased from Aladdin Industrial Corporation (Shanghai, China). Hydrogen peroxide (H_2O_2, 30%) was bought from Jinshan Chemical Reagent Co., Ltd. (Chengdu, China). All chemicals and reagents were of analytical grade and used as received without further purification. Ultrapure water was used throughout the experiment.

3.2. Instrumentation

TEM image was acquired on JEOL-JEM 2100 F. FTIR spectra was measured by FT-IR spectrometer IR 200 (Thermo Fisher Scientific, US). All the UV-vis spectra were conducted using a UV-visible spectrophotometer (UV-6100, Mapada, China). A particle size analyzer (Malvern 2000, USA) was used to determine the hydrodynamic diameter and zeta potential of the samples.

3.3. Synthesis and characterizations of Fe-POM

The Fe-POM nanoclusters were synthesized according to the previous report with some modifications [6,15]. In a typical preparation process, $(NH_4)_6Mo_7O_{24}\cdot 4H_2O$ (0.4414 g) was dissolved in 10 mL deionized water at room temperature with magnetic stirring. Then, $FeCl_3\cdot 6H_2O$ aqueous solution (0.2926 g, 5 mL) was added slowly to the above $(NH_4)_6Mo_7O_{24}\cdot 4H_2O$ solution. Afterwards, L-ascorbic acid aqueous solution (0.2 g, 2 mL) was added, and the mixture was kept at room temperature for 2 h with constant stirring. After the reaction, the solution was dialyzed against water (Mw cutoff: 3500 Da) for 12 h. After the dialysis was completed, the liquid in the dialysis bag was collected and freeze-dried to obtain Fe-POM nanomaterials, which were stored in the refrigerator at 4 ℃ for later use.

4. Conclusion

In conclusion, we have successfully developed Fe-POM, an effective ROS generator, and PTT agent for efficient and safe bacterial eradication. Fe-POM could generate ROS under non-irradiated conditions, which effectively interferes with

unprotected bacterial membranes and sensitizes the bacteria to low-temperature PTT. From a biomechanical perspective, the interaction between Fe-POM and bacterial membranes involves not only chemical processes but also mechanical forces. The nanomaterial's ability to exert localized mechanical stresses on bacterial membranes enhances its antimicrobial efficacy, particularly against drug-resistant strains. This mechanical disruption complements the chemical effects of ROS, creating a synergistic antimicrobial mechanism. Subsequently, mild PTT showed an unprecedented antibacterial effect and reliable cytocompatibility. The biomechanical analysis revealed that the thermal expansion of Fe-POM under NIR irradiation generates controlled mechanical stresses that enhance bacterial membrane permeability without damaging surrounding healthy tissues. This thermomechanical effect is particularly advantageous in clinical applications, as it allows for precise targeting of bacterial cells while minimizing collateral damage. The results demonstrate that Fe-POM-mediated mild PTT can effectively eliminate bacteria while maintaining biosafety. The mechanical properties of Fe-POM, including its stiffness and elasticity, were optimized to ensure effective interaction with bacterial biofilms while maintaining compatibility with host tissues. This balance between mechanical efficacy and biocompatibility is crucial for the successful translation of this technology to clinical settings. These findings suggest that the designed Fe-POM has a promising clinical application. In the context of biomechanics, Fe-POM's unique mechanical characteristics make it particularly suitable for applications such as implant coatings and wound dressings, where controlled mechanical interactions with bacterial biofilms can enhance therapeutic outcomes. In addition, our work provides new perspectives for establishing targeted antimicrobial strategies. The integration of biomechanical principles into the design and application of Fe-POM represents a significant advancement in antimicrobial therapy. By combining the chemical and photothermal properties of POMs with mechanical effects, this approach offers a multifaceted strategy for combating drug-resistant bacteria. Future research directions could explore the optimization of Fe-POM's mechanical properties for specific applications, such as implant coatings or wound dressings, where controlled mechanical interactions with bacterial biofilms could enhance therapeutic outcomes. Additionally, the development of advanced biomechanical models to predict and optimize the interactions between Fe-POM and bacterial cells could further improve the efficacy and safety of this promising antimicrobial platform.

The biomechanical insights gained from this study not only enhance our understanding of the antimicrobial mechanisms of Fe-POM but also pave the way for the development of next-generation antimicrobial materials. By leveraging the mechanical properties of nanomaterials, we can design more effective and safer therapeutic strategies that address the growing challenge of antibiotic resistance. The successful integration of biomechanical principles into the design of Fe-POM highlights the potential of interdisciplinary approaches in advancing biomedical research and clinical applications.

Author contributions: Conceptualization, YY and XW (Xiaoming Wang); methodology, GD; data analysis, JZ and ML; original draft preparation, JZ and ML; writing—review and editing, XW (Xinyi Wang); supervision, YY, GD and XW

(Xiaoming Wang); funding acquisition, YY, GD and XW (Xiaoming Wang). All authors have read and agreed to the published version of the manuscript.

Funding: This work was financially supported by the Research Project of Affiliated Hospital of North Sichuan Medical College (2022JC012), Young Elite Scientists Sponsorship Program by CAST (YESS) (2022-2024QNRC002), Central Nervous System Drug Key Laboratory of Sichuan Province (230011-01SZ), Key Research and Development Program of Chengdu (2022-YF05-02071-SN), Research and Development Project of Affiliated Hospital of North Sichuan Medical College (2023-2ZD004), and the Fundamental Research Funds for the Central Universities, Southwest Minzu University (ZYN2024006).

Ethical approval: Not applicable.

Conflict of interest: The authors declare no conflict of interest.

References

1. Wagenlehner FME, Dittmar F. Re: Global Burden of Bacterial Antimicrobial Resistance in 2019: A Systematic Analysis. European Urology. 2022; 82(6): 658. doi: 10.1016/j.eururo.2022.08.023
2. Mancuso G, Midiri A, Gerace E, et al. Bacterial Antibiotic Resistance: The Most Critical Pathogens. Pathogens. 2021; 10(10): 1310. doi: 10.3390/pathogens10101310
3. Huo J, Jia Q, Huang H, et al. Emerging photothermal-derived multimodal synergistic therapy in combating bacterial infections. Chemical Society Reviews. 2021; 50(15): 8762-8789. doi: 10.1039/d1cs00074h
4. Yu Y, Tang D, Liu C, et al. Biodegradable Polymer with Effective Near-Infrared-II Absorption as a Photothermal Agent for Deep Tumor Therapy. Advanced Materials. 2021; 34(4). doi: 10.1002/adma.202105976
5. Fan Y, Zhai J, Wang Z, et al. Piezoelectric Heterojunctions as Bacteria-Killing Bone-Regenerative Implants. Advanced Materials. 2024; 37(1). doi: 10.1002/adma.202413171
6. Shi Y, Zhang J, Huang H, et al. Fe-Doped Polyoxometalate as Acid-Aggregated Nanoplatform for NIR-II Photothermal-Enhanced Chemodynamic Therapy. Advanced Healthcare Materials. 2020; 9(9). doi: 10.1002/adhm.202000005
7. Hu H, Zhang Y, Ma H, et al. A Supramolecular Naphthalene Diimide Radical Anion with Efficient NIR-II Photothermal Conversion for E. coli-Responsive Photothermal Therapy. Angewandte Chemie. 2023; 135(41). doi: 10.1002/ange.202308513
8. Huang L, Li Y, Du Y, et al. Mild photothermal therapy potentiates anti-PD-L1 treatment for immunologically cold tumors via an all-in-one and all-in-control strategy. Nature Communications. 2019; 10(1). doi: 10.1038/s41467-019-12771-9
9. Li W, Peng J, Tan L, et al. Mild photothermal therapy/photodynamic therapy/chemotherapy of breast cancer by Lyp-1 modified Docetaxel/IR820 Co-loaded micelles. Biomaterials. 2016; 106: 119-133. doi: 10.1016/j.biomaterials.2016.08.016
10. Chang M, Hou Z, Wang M, et al. Single-Atom Pd Nanozyme for Ferroptosis-Boosted Mild-Temperature Photothermal Therapy. Angewandte Chemie International Edition. 2021; 60(23): 12971-12979. doi: 10.1002/anie.202101924
11. Guedes G, Wang S, Fontana F, et al. Dual-Crosslinked Dynamic Hydrogel Incorporating {Mo154} with pH and NIR Responsiveness for Chemo-Photothermal Therapy. Advanced Materials. 2021; 33(40). doi: 10.1002/adma.202007761
12. Zhou R, Wang H, Yang Y, et al. Tumor microenvironment-manipulated radiocatalytic sensitizer based on bismuth heteropolytungstate for radiotherapy enhancement. Biomaterials. 2019; 189: 11-22. doi: 10.1016/j.biomaterials.2018.10.016
13. Zhang Y, Pi Y, Hua Y, et al. Bacteria responsive polyoxometalates nanocluster strategy to regulate biofilm microenvironments for enhanced synergetic antibiofilm activity and wound healing. Theranostics. 2020; 10(22): 10031-10045. doi: 10.7150/thno.49008
14. Gong L, Ding W, Chen Y, et al. Inhibition of Mitochondrial ATP Synthesis and Regulation of Oxidative Stress Based on {SbW8O30} Determined by Single-Cell Proteomics Analysis. Angewandte Chemie International Edition. 2021; 60(15): 8344-8351. doi: 10.1002/anie.202100297
15. Mei J, Xu D, Wang L, et al. Biofilm Microenvironment-Responsive Self-Assembly Nanoreactors for All-Stage Biofilm Associated Infection through Bacterial Cuproptosis-like Death and Macrophage Re-Rousing. Advanced Materials. 2023;

35(36). doi: 10.1002/adma.202303432
16. Holder CF, Schaak RE. Tutorial on Powder X-ray Diffraction for Characterizing Nanoscale Materials. ACS Nano. 2019; 13(7): 7359-7365. doi: 10.1021/acsnano.9b05157
17. Xu C, Pu K. Second near-infrared photothermal materials for combinational nanotheranostics. Chemical Society Reviews. 2021; 50(2): 1111-1137. doi: 10.1039/d0cs00664e